The UCLA Coupled Atmosphere-Ocean GCM Simulation of the Surface Heat Flux in the Tropical Pacific

Jin-Yi Yu, Carlos R. Mechoso, and Chung-Chun Ma

Department of Atmospheric Sciences
University of California, Los Angeles
Los Angeles, California, USA

1 Introduction

In a coupled atmosphere-ocean general circulation model (CGCM, hereafter), the atmospheric component (AGCM) and the oceanic component (OGCM) interact through the exchange of SST and surface fluxes of heat, momentum, and fresh water. The deficiencies in the CGCM, therefore, depend in a complicated way on the deficiencies in the individual model components due to the feedbacks in the coupled atmosphere-ocean system. One method to gain insight into the behavior of the CGCM is to compare the errors in the coupling fields produced by the CGCM and by each one of its components running with prescribed boundary conditions. In this paper we focus on the surface heat flux, and compare the corresponding fields for the Tropical Pacific produced by the UCLA CGCM, the UCLA uncoupled AGCM, and those compiled in Oberhuber (1988) by using observational data.

2 Model description

The version of the UCLA CGCM used in this study consists of a global atmospheric model and a Tropical Pacific oceanic model. The atmospheric component is a 9-layer and 4°-latitude by 5°-longitude version of the UCLA AGCM (Suarez et al. 1983 and references therein). The oceanic component is the GFDL OGCM (Bryan 1969 and Cox 1984). The domain of the OGCM extends from 30°S to 50°N and from 130°W to 70°E. Mean seasonal cycles of surface heat fluxes are calculated from a 9-year CGCM simulation and a 4-year uncoupled AGCM simulation. The latter simulation uses time-varying SST from an observed climatology.

3 Surface heat flux and SST

The annual-mean surface heat fluxes from the CGCM and AGCM simulations and the observational estimate are shown in Figure 1. The major features of surface heat flux in the observational estimate are obtained in both simulations. The magnitudes of the surface heat flux in the AGCM simulation, however, are too large in the subtropics of both hemispheres and off the coasts of North and South America. The surface heat flux simulated with the CGCM appears to be more realistic. The root-mean-square errors, in reference to the observational estimates, are calculated for the

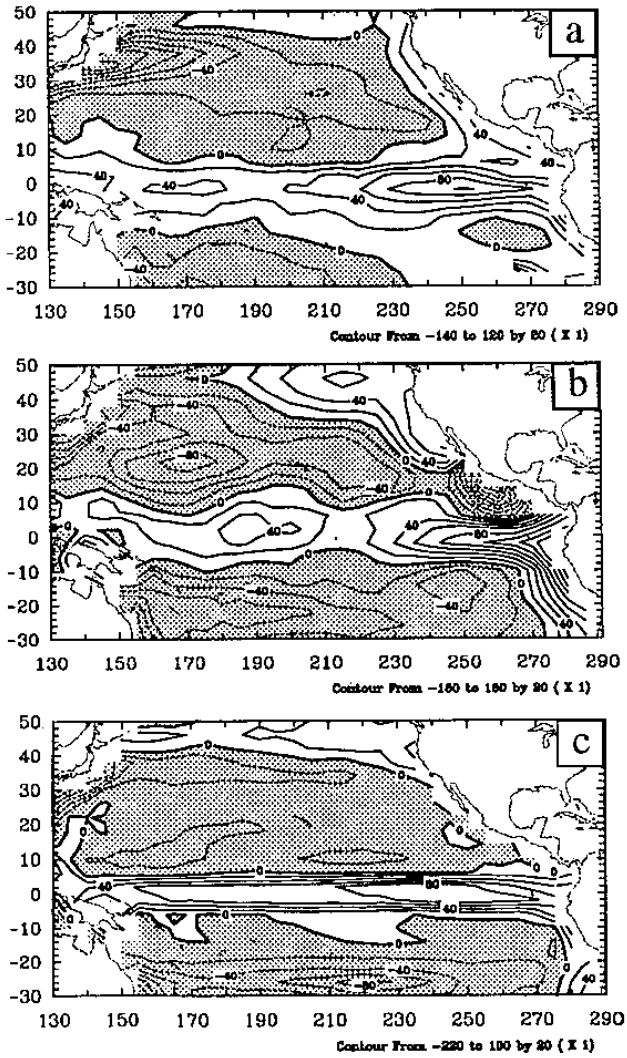

Figure 1. Annual-mean surface heat flux from (a) Oberhuber's estimate, (b) AGCM and (c) CGCM simulations. Fluxes out of the ocean are shaded. The contour interval is 20 W/m**2.

seasonal cycles of surface heat flux obtained from the model simulations. The differences between the errors in the CGCM and AGCM simulations are shown in Figure 2. This figure shows that except in the equatorial Pacific, the root-mean-square errors are smaller in the CGCM simulation than in the AGCM simulation. This suggests that the seasonal cycle of surface heat simulated with the CGCM is also more realistic than that with the uncoupled AGCM.

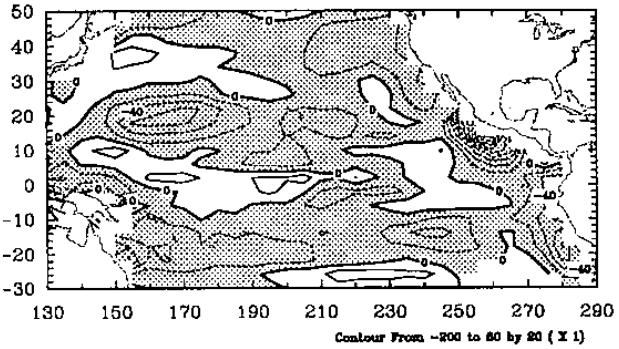

Figure 2. The differences between the root-mean-square errors in the seasonal cycle of the surface heat flux simulated with the CGCM and those simulated with the uncoupled AGCM. Differences less than zero are shaded and indicate the errors are smaller in the CGCM simulation than in the AGCM simulation. Contour interval is 20 W/m**2.

Since the AGCM simulation used observed SSTs, we do not expect *a priori* more realistic surface heat flux with the CGCM than that with the uncoupled AGCM. The AGCM deficiencies that result in surface heat flux errors in the uncoupled AGCM simulation, therefore, must have been compensated by the ocean model in the CGCM simulation. To examine this hypothesis, we contrast the root-mean-square errors of SST in the CGCM simulation along with the root-mean-square surface heat flux difference between the CGCM and AGCM simulations (see Figure 3). It is apparent that five of the six regions of maximum SST error in the CGCM simulation coincide with regions of large surface heat flux difference between the coupled and uncoupled simulations. Only the SST error maximum in the eastern equatorial Pacific does not have a counterpart in the surface heat flux difference.

The errors in the annual-mean SST from the CGCM simulation and that in the annual-mean surface heat flux from the AGCM simulation are shown in Figure 4. This figure suggests that the SST errors in the CGCM simulation compensate the AGCM deficiency in surface

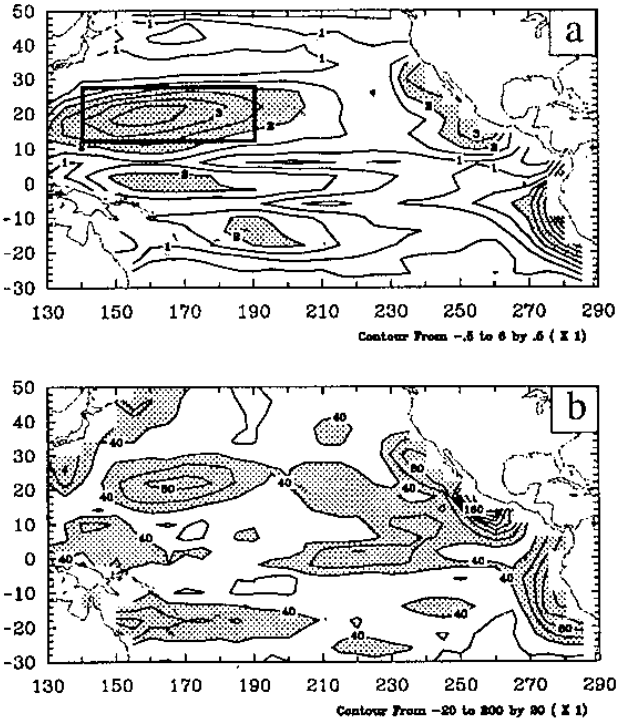

Figure 3. (a) Root-mean-square SST errors in the CGCM simulation, and (b) root-mean-square surface heat flux difference between the CGCM and AGCM simulations. Errors greater than 2°K in (a) and differences greater than 40W/m**2 in (b) are shaded. The contour interval is 0.5°K for (a) and 20 W/m**2 for (b).

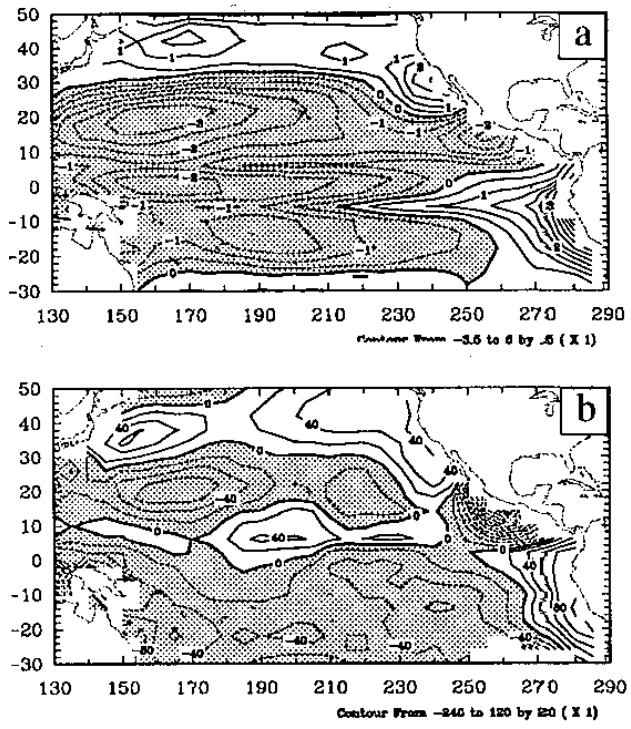

Figure 4. The errors in the annual-mean (a) SST simulated with the CGCM and (b) surface heat flux simulated with the uncoupled AGCM The contour interval is 0.5°K for (a) and 20 W/m**2 for (b).

heat flux. Except in the equatorial region, the simulated SSTs have a cold (warm) bias in the locations where the surface heat fluxes simulated with the uncoupled AGCM are too weak (strong). To inspect more closely the spatial coincidence shown in Figure 3, the seasonal variations of the SST errors in the CGCM simulation and the surface heat flux difference between two model simulations are compared in Figure 5 for the region identified by an rectangle in Figure 3a. Figure 5 shows that the increase (decrease) of SST error in this region is accompanied with larger (smaller) surface heat flux difference. These results, therefore, support the hypothesis that the reduction of surface heat flux errors in the off-equatorial regions of the CGCM simulation is achieved at the expense of errors in SST.

To narrow down on the physical processes primarily responsible for the reduction in surface heat flux errors and the increase in SST errors in the CGCM simulation, we have compared the latent heat and net radiation fluxes simulated by the CGCM and the uncoupled AGCM for those six regions of large SST errors. The comparisons (not shown) reveals that the major contributor to the error in the surface heat flux simulated with the uncoupled AGCM is the error in the latent heat flux. In the CGCM simulation, on the other hand, the cold-bias in SST reduces evaporation and brings surface heat flux closer to the observational estimate in most regions. Off the coasts of Peru and California, the main cause of surface heat flux errors is the too strong net radiation into the ocean. The CGCM produces a warm SST bias in these two regions, which further increases the already too strong evaporation to reduce the magnitude of surface heat flux into the ocean. In summary, the major AGCM deficiencies in surface heat flux is the evaporation process in the subtropics of both hemispheres and the radiation processes along the eastern part of the Tropical Pacific.

4 Surface heat flux simulation in the equatorial Pacific

In this section we focus on the surface heat flux simulated over the equatorial Pacific. The seasonal cycles of surface heat flux over the western and the eastern equatorial Pacific are shown in Figure 6 for the CGCM and AGCM simulations and the observational

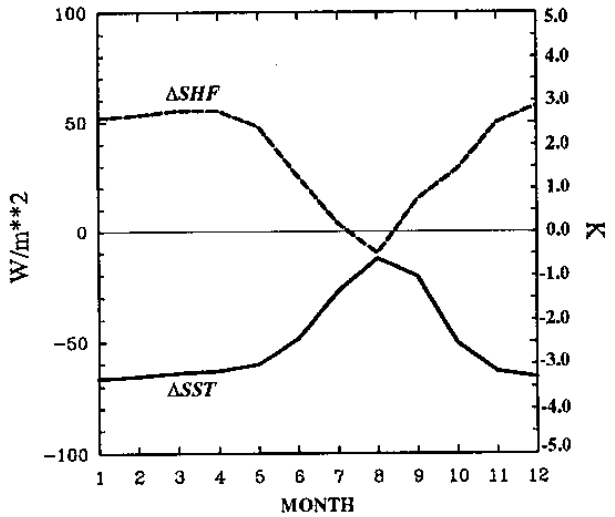

Figure 5. Seasonal variations of the SST errors (solid-line) in the CGCM simulation and the surface heat flux errors (dashed-line) in the AGCM simulation for the rectangle region identified in Figure 3a.

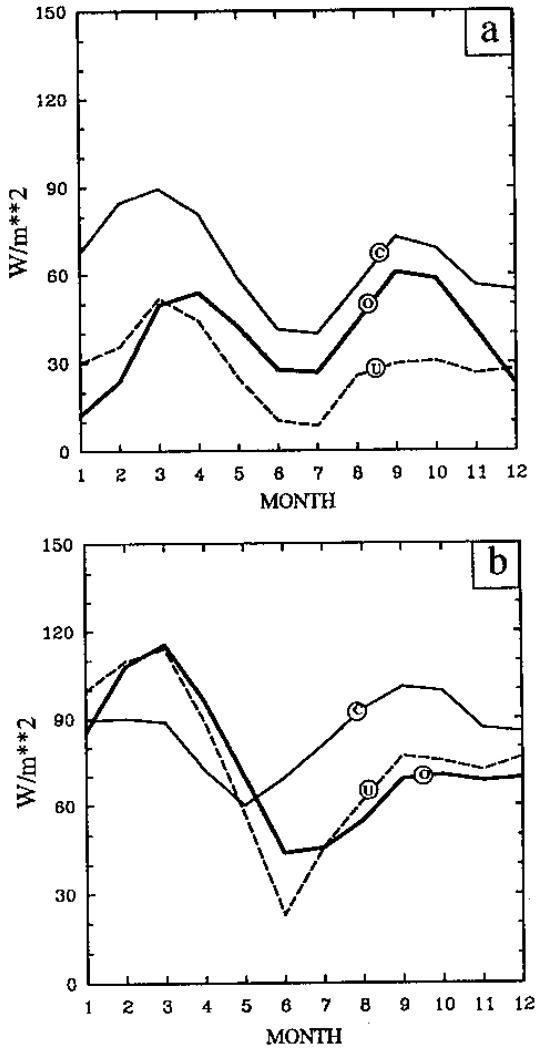

Figure 6. Seasonal cycles of surface heat flux averaged over (a) the western Equatorial Pacific and (b) the eastern Equatorial Pacific from the Oberhuber estimate (indicated by "O") and the CGCM ("C") and AGCM ("U") simulations.

estimate. Over the western equatorial Pacific, both the CGCM and the uncoupled AGCM produce similar seasonal variations in the surface heat flux. The larger surface heat flux errors in the CGCM simulation (see Figure 2) are mainly due to the too large annual-mean. As for the eastern equatorial Pacific, the uncoupled AGCM produces a better simulation on the seasonal cycle of surface heat flux than the CGCM. The larger surface heat flux errors in the CGCM simulation are associated with phase errors in the seasonal cycle. Further analyses have suggested that this phase error is linked to the seasonal variation of latent heat flux. Figure 7 shows the seasonal cycles of latent heat flux for the model simulations and the observational estimate. It is apparent that the seasonal variation of the latent heat flux simulated with the CGCM is almost in opposition phase to that in the observational estimate and that simulated with the uncoupled AGCM.

In both the Oberhuber's estimates and the model simulations, the parameterizations of surface latent heat flux are based on the bulk-aerodynamic formula:

$$L = C \cdot V \cdot \Delta q \qquad (1)$$

where V is wind speed, Δq the difference between the mixing ratios on the ocean surface and the overlying air, and C is the transfer coefficient. If annual-means and seasonal deviations are indicated by overbars and

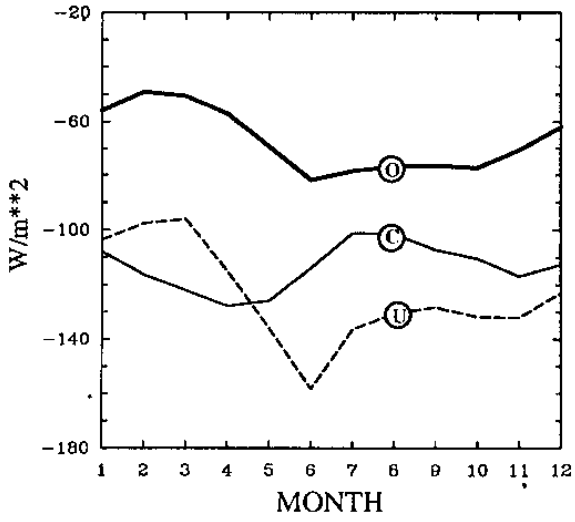

Figure 7. Seasonal cycles of surface latent heat flux averaged over the eastern equatorial Pacific from the Oberhuber estimate (thick solid-line) and the CGCM (solid-line) and AGCM (dash-line) simulations.

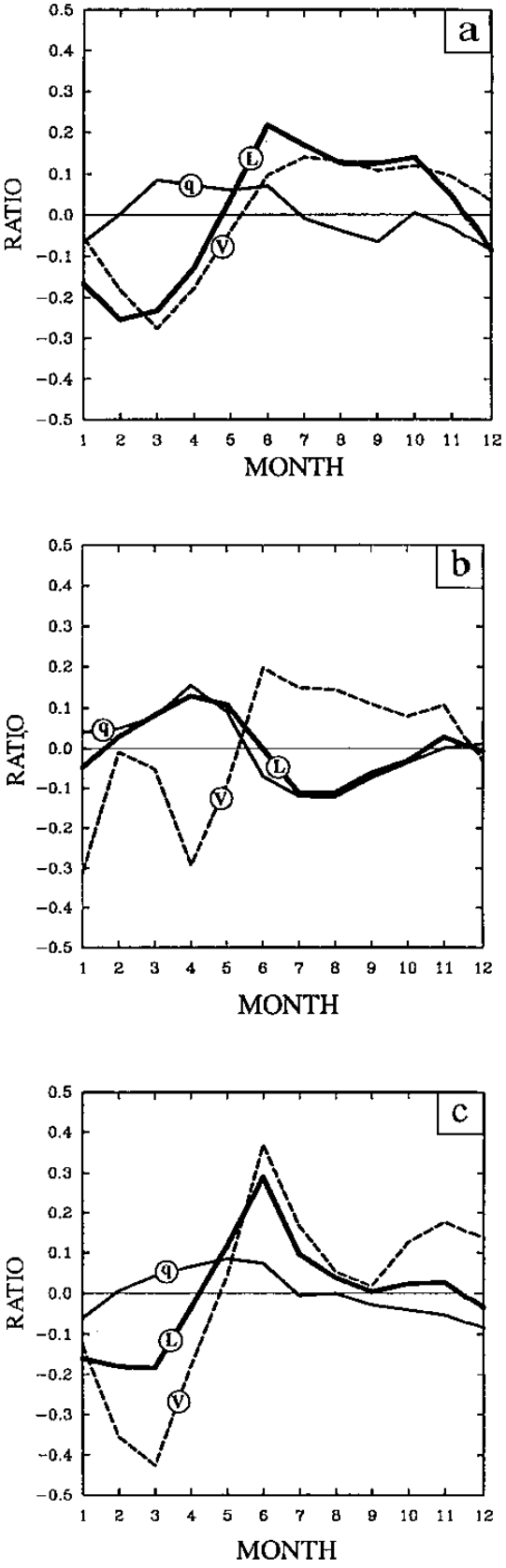

Figure 8. Contributions to the seasonal variations of latent heat flux from the wind speed term and humidity difference term of equation (4) in (a) the Oberhuber estimate and (b) the CGCM and (c) AGCM simulations. The characters "L" indicate the seasonal variations of the term $L'/\overline{L}$ in Equation (4), "q" for the term $(\Delta q)'/\overline{\Delta q}$, and "V" for the term $V'/\overline{V}$.

primes in the equation for each quantity in that equation, the seasonal deviation form of Equation (1) can be approximated by the following relationship:

$$L' \approx C' \cdot \overline{V} \cdot \overline{\Delta q} + \overline{C} \cdot V' \cdot \overline{\Delta q} + \overline{C} \cdot \overline{V} \cdot (\Delta q)' \,. \qquad (2)$$

Since

$$L \approx \overline{C} \cdot \overline{V} \cdot \overline{\Delta q} \,, \qquad (3)$$

equation (2) can be further simplified to:

$$\frac{L'}{L} \approx \frac{C'}{\overline{C}} + \frac{V'}{\overline{V}} + \frac{(\Delta q)'}{\overline{\Delta q}} \,. \qquad (4)$$

We use Equation (4) to estimate the relative importance of wind speed, humidity difference, and transfer coefficient in determining the seasonal variation of surface latent heat flux over the eastern equatorial Pacific.

Figure 8 shows the seasonal variations of the terms L'/L, $V'/\overline{V}$ and $(\Delta q)'/\overline{\Delta q}$ in equation (4) for the CGCM and AGCM simulations and the observational estimate. The transfer coefficient C is not stored in the model output and is difficult to obtain from the history files. For this reason, the contribution from this term is treated as the residual of equation (4) and is not shown. Figure 8a shows that the seasonal deviation of the wind speed in the observational estimates is out of phase with the humidity difference. A similar out-of-phase relation between the seasonal anomalies in wind speed and humidity difference is obtained in the CGCM simulation. The surface latent heat flux in Oberhuber's estimate has a seasonal variation similar to that of the wind speed, while the surface latent heat flux simulated with the CGCM has a seasonal variation similar to that of the humidity difference. Thus, the latent heat flux simulated with the CGCM exhibits a seasonal variation that is almost in opposition of phase with the observational estimate. The seasonal variation of transfer coefficient in the CGCM simulation must be, therefore, in opposition of phase to that in Oberhuber's estimate. For the uncoupled AGCM, the seasonal variation of latent heat flux is closer to that of the wind speed than to the humidity difference. Further analyses are needed to clarify why in the CGCM the humidity difference has a stronger influence on the seasonal cycle of latent heat flux than the wind speed.

5 Summary

This study shows that the surface heat flux simulated with the CGCM in the Tropical Pacific away from the equator is closer to the observational estimates than that with the uncoupled AGCM, and that this improvement is obtained at the expense of errors in SST. The results also suggest that the AGCM deficiencies in surface heat flux are related to the local SST errors in the off-equatorial regions of the tropical Pacific in the CGCM simulation. Surface heat flux errors caused by those deficiencies are compensated in the GCM simulation with SST errors through the evaporation process.

These features in the simulation of surface heat flux are different from those in the equatorial region. The surface heat flux errors at the equator have larger magnitudes in the CGCM simulation than that in the AGCM simulation. The larger surface heat flux errors in the CGCM simulation at the equator is associated with an excessively large annual-mean over the western Pacific and with a phase error in the seasonal cycle over the eastern Pacific.

Acknowledgments. The authors benefit from discussions with Professor A. Arakawa and Dr. A. W. Robertson. This work was supported by NASA under Grant NAG5-2224, by DOE/CHAMMP under Grant DE-FG03-91ER61214 A004, and by INCOR. Model integrations were performed at the San Diego Supercomputer Center.

References

Bryan, K., 1969: A numerical method for the study of the circulation of the world ocean. *J. Comp. Phys.*, 4, 347-376.

Cox, M.D., 1984: A primitive equation three-dimensional model of the ocean. GFDL Ocean Group Tech. Rep. Non.1.

Oberhuber, J.M., 1988: An atlas based on the COADS data set: the budgets of heat buoyancy and turbulent kinetic energy at the surface of the global ocean. Max-Plank-Institut für meteorologie Report No. 15, Bundesstrasse 55, 2000 Hamburg 13, FRG.

Suarez, M.J., A. Arakawa, and D.A. Randall, 1983: The parameterization of the planetary boundary layer in the UCLA general circulation model: Formulation and results. *Mon. Wea. Rev.*, 111, 2224-2243.